Int Urogynecol J (2017) 28:1131–1138
DOI 10.1007/s00192-017-3263-1

ORIGINAL ARTICLE

MRI visible Fe_3O_4 polypropylene mesh: 3D reconstruction of spatial relation to bony pelvis and neurovascular structures

Luyun Chen[1] · Florian Lenz[2] · Céline D. Alt[3] · Christof Sohn[4] · John O. De Lancey[5] · Kerstin A. Brocker[4]

Received: 10 November 2016 / Accepted: 3 January 2017 / Published online: 25 January 2017

Abstract
Introduction and hypothesis To demonstrate mesh magnetic resonance imaging (MRI) visibility in living women, the feasibility of reconstructing the full mesh course in 3D, and to document its spatial relationship to pelvic anatomical structures.
Methods This is a proof of concept study of three patients from a prospective multi-center trial evaluating women with anterior vaginal mesh repair using a MRI-visible Fe_3O_4 polypropylene implant for pelvic floor reconstruction. High-resolution sagittal T2-weighted (T2w) sequences, transverse T1-weighted (T1w) FLASH 2D, and transverse T1w FLASH 3D sequences were performed to evaluate Fe_3O_4 polypropylene mesh MRI visibility and overall post-surgical pelvic anatomy 3 months after reconstructive surgery. Full mesh course in addition to important pelvic structures were reconstructed using the 3D Slicer® software program based on T1w and T2w MRI.
Results Three women with POP-Q grade III cystoceles were successfully treated with a partially absorbable MRI-visible anterior vaginal mesh with six fixation arms and showed no recurrent cystocele at the 3-month follow-up examination. The course of mesh in the pelvis was visible on MRI in all three women. The mesh body and arms could be reconstructed allowing visualization of the full course of the mesh in relationship to important pelvic structures such as the obturator or pudendal vessel nerve bundles in 3D.
Conclusions The use of MRI-visible Fe_3O_4 polypropylene meshes in combination with post-surgical 3D reconstruction of the mesh and adjacent structures is feasible suggesting that it might be a useful tool for evaluating mesh complications more precisely and a valuable interactive feedback tool for surgeons and mesh design engineers.

Keywords 3D mesh reconstruction · Fe_3O_4 · MRI-visible anterior mesh · Pelvic floor mesh surgery · Pelvic organ prolapse

Electronic supplementary material The online version of this article (doi:10.1007/s00192-017-3263-1) contains supplementary material, which is available to authorized users

✉ Kerstin A. Brocker
kerstin.brocker@med.uni-heidelberg.de

[1] Pelvic Floor Research Group, Biomedical Engineering Department, University of Michigan, 2350 Hayward Street, Ann Arbor, MI 48103, USA

[2] Department of Obstetrics and Gynecology, St Marienkrankenhaus Ludwigshafen, Academic Teaching Hospital of the Faculty of Medicine Mannheim of the University Medical School Heidelberg, Salzburgerstrasse 15, 67067 Ludwigshafen am Rhein, Germany

[3] Medical Faculty, Department of Diagnostic and Interventional Radiology, University Düsseldorf, Moorenstrasse 5, 40225 Düsseldorf, Germany

[4] Medical School, Department of Obstetrics and Gynecology, University of Heidelberg, Im Neuenheimer Feld 440, 69120 Heidelberg, Germany

[5] Obstetrics and Gynecology Department, Pelvic Floor Research Group, University of Michigan, Ann Arbor, MI 48103, USA

Introduction

Pelvic organ prolapse is a distressing condition that requires surgery in over 200,000 women each year in the USA, a number that is expected to substantially increase in the coming decades [1–3]. Besides the performance of classic urogynecological surgery techniques, the use of synthetic material for pelvic organ prolapse (POP) repair has been established over the past few decades. Synthetic transvaginal mesh was permanently implanted to reinforce the weakened

vaginal wall for POP repair, usually with arms anchored in structures near the pelvic side wall. However, surgery outcome results have shown heterogeneous data in terms of mesh erosions, post-surgical pain, and dyspareunia or recurrent prolapse [4, 5].

Visualizing the mesh can be helpful in evaluating patients with mesh complications. 2D, 3D/4D ultrasound has proved to be useful in visualizing mesh adjacent to the vagina, demonstrating folding or inappropriate positioning of the implant, and assessing vaginal mobility in relationship to the mesh location [6–8]. It is difficult, however, to visualize the entire mesh, including the course of the arms through deep body structures such as the obturator neurovascular bundle or the sacrospinous ligament and the pudendal neurovascular structures. To achieve full mesh visualization in the female pelvis a MRI-visible mesh was developed, applying an iron compound onto the mesh material, for iron has been previously shown to be visible with some MRI sequences [9–11]. The newly developed MRI-visible Fe_3O_4 polypropylene mesh has demonstrated MRI visibility in a cadaver study [9]. Whether or not the fine mesh structure could be seen in living women, in whom tissue movement from vascular pulsation, breathing, and muscle activity might reduce visibility, is not known.

As a proof of concept study, the goals are to:

1. Describe the technique
2. Assess the mesh MRI visibility in living women
3. Demonstrate the feasibility of reconstructing the full course of the mesh
4. Visualize the mesh's spatial relationship to important pelvic floor anatomical structures, for example, if the mesh is invading any surround organ or whether it is close to blood vessels or nerve bundles.

This valuable information could potentially aid clinical diagnosis and revision surgery planning.

Materials and methods

Study design

This is a proof of concept study of three patients from an ongoing prospective multi-center clinical trial (ethical board reference number: S-473/2007, amendment 9 July 2015) to observe and evaluate women with anterior vaginal mesh repair using a magnetic resonance imaging (MRI)-visible Fe_3O_4 polypropylene implant. All women participating in this examination matched the inclusion criteria (symptomatic grade ≥ 2 cystocele with apical prolapse scheduled for anterior mesh surgery with apical fixation through the sacrospinous ligaments, no contraindication for surgery or MRI, age ≥ 18 years) and gave their written informed consent. Exclusion criteria were vaginal reconstructive surgery without anterior mesh, general contraindications for surgery or MRI, age ≤ 18 years).

Mesh information and implantation

Partially absorbable (PA) anterior vaginal meshes (Seratom® E PA MR or Seratom® P PA MR by Serag Wiessner, Naila, Germany) were implanted. These meshes have six fixational arms, of which the posterior arms are fixed in the sacrospinous ligaments, whereas the middle and anterior arms are placed via the obturator muscle membrane complex [12]. The non-absorbable material is MRI-visible, as described in our previous study [9]. The two meshes (Seratom® E PA MRI being 6 x 10 cm and the Seratom® P PA MR 4 x 9 cm) differ only in size/shape. The MRI visibility of this alloplastic material is created with a defined concentration of (0.2 weight %) Fe_3O_4 added to the polypropylene—unlike other MRI-visible meshes on the market that integrate paramagnetic Fe_3O_4 microparticles into polyvinylidene fluoride (PVDF) polymer filaments [9, 13]. The MRI-visible meshes produced by Serag Wiessner have been on the clinical market with CE certification since 2013. The implantation of the mesh was performed according to the company recommendations with the help of the mesh implantation tools (multi-incision trocar-guided technique with reusable introducers/needles) [12]. The anterior and middle arms were placed through the obturator foramen, and the posterior arms penetrated the sacrospinous ligament on both sides and passed outward through the ischio-anal fossa [12].

Magnetic resonance imaging

All patients underwent a pre- and post-surgical (10–12 weeks after surgery) MRI with a moderately filled bladder in a 1.5-Tesla scanner (Siemens Symphony, Siemens Medical Solutions, Erlangen, Germany). Sterile gel (Endosgel®) was inserted into the vagina to ensure better visualization of the vaginal walls [14]. All images were obtained in the supine position. The examination protocol included high-resolution sagittal T2-weighted (T2w) turbo-spin-echo (TSE) sequence for morphological visualization of the pelvic tissues and organs (TR 3,460–4,219 ms, TE 77–85 ms, slice thickness 5 mm, matrix 512 × 282) and transverse T2w TSE sequence (TR 3,460 ms, TE 88 ms, slice thickness 6 mm, matrix 512 × 282). To delineate the mesh structures, a transverse T1-weighted (T1w) FLASH 2D (fl2D) sequence (TR 128–132 ms, TE 4.7 ms, slice thickness 6 mm, matrix 256 × 154) and a transverse T1w FLASH 3D (fl3D) sequence (TR 15.0 ms, TE 6.0 ms, slice thickness 1 mm, matrix 512 × 384) was performed. In this scan the threads of the mesh containing Fe_3O_4 particles demonstrate hypointense signal due to circumscribed susceptibility artifacts. The field of view (FOV) of the sequences covered the entire pelvis including the

promontory and the pelvic floor. Only post-surgical MR images were analyzed in this study.

Mesh and pelvic structure 3D reconstruction

The three-dimensional (3D) reconstruction of the mesh implant and the neighboring anatomical structures was performed using the 3D Slicer® software program (version 4.3.1–2) and the original Digital Imaging and Communications in Medicine (DICOM) static MR images of the above-mentioned sequences [15]. First, bony landmarks such as inferior-most pubic symphysis, ischial spines, and sacrococcygeal junction (SCJ) were identified on T1w and T2w images [16]. These landmarks were used to align different MRI sequences in the same 3D space. The pelvic bone, in addition to organs and ligaments, were manually traced from T2w images in all slices in which they could be identified and then 3D volume rendering models were reconstructed.

The mesh was identified on T1w fl2D and fl3D images as small hypointense, "dark" spots compared with surrounding tissues on T1w images. Fiducials, single point identifiers, were placed on these locations to produce a "cloud" of visible points and confirmed in all three projection views (transverse, coronal, and sagittal) as well as in 3D space (Fig. 1). This "point cloud" technique [17] was applied rather than the 3D volume-rendered models to avoid the lofting and smoothing errors introduced by computer algorithms used for model reconstruction and because point placement was more precise than the line drawing needed for model construction. Using the same technique, important anatomical structures such as obturator vessels and pudendal neurovascular bundles were reconstructed based on T1w and T2w images to demonstrate their relationship with implanted mesh.

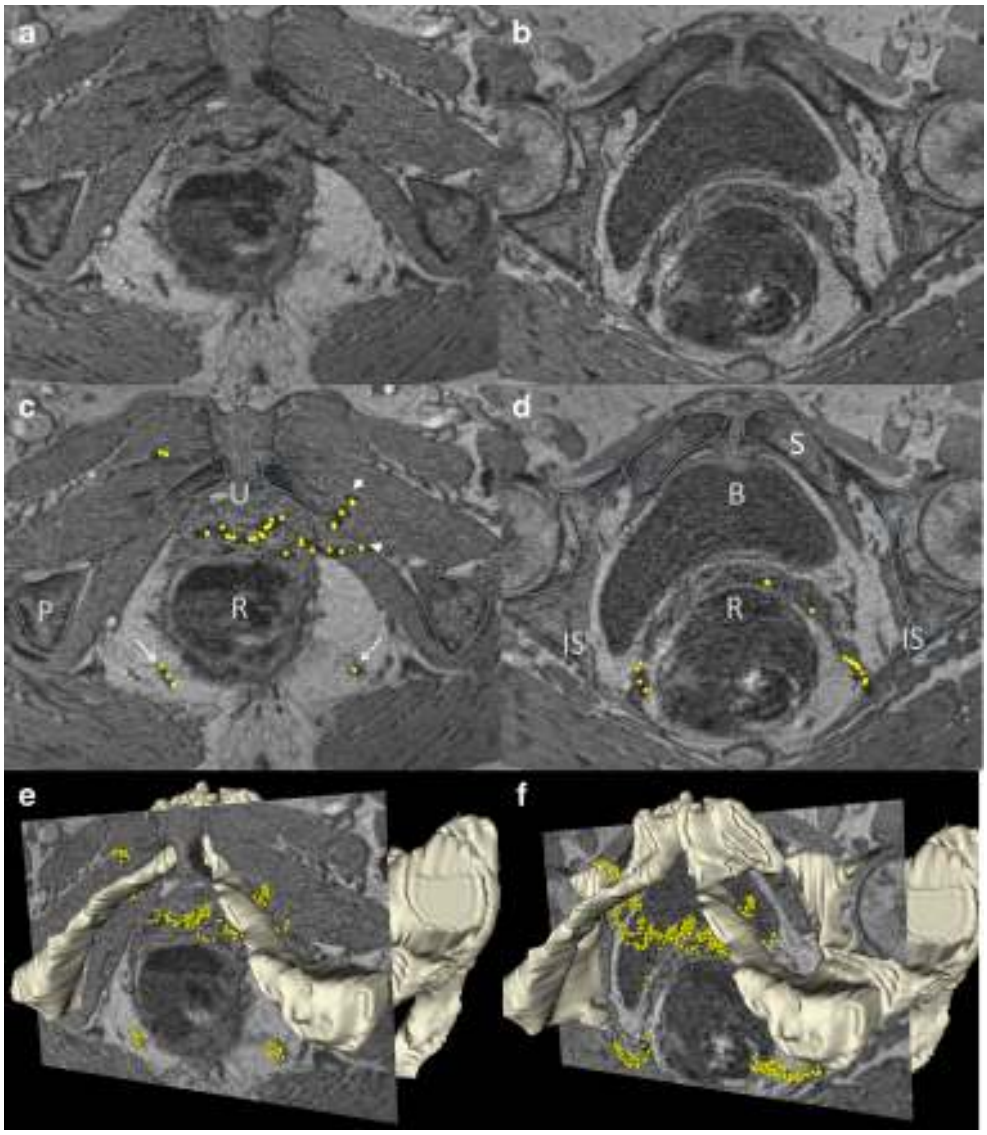

Fig. 1 Creation of 3D Slicer model from the transverse planes. T1-weighted FLASH 3D (T1w fl3D) sequence, with **a**, **c**, and **e** at the level of the mid-urethra (*U*) and **b**, **d**, and **f** at the level of the bladder (*B*) in patient 1 after anterior compartment repair using a six-arm Fe_3O_4 polypropylene mesh. **a, b** are unlabeled original MR images. **c, d** The visible mesh is marked with *yellow dots* in the two-dimensional view. **e, f** show the tilted 3D model of the pelvis (*P*) and the location of the implanted mesh with the MRI images **a** and **b** for better spatial evaluation and understanding. In **a** and **c** the distal part of the mesh body can be seen beneath the urethra, in addition to the left anterior and middle arms (*arrowheads* in **c**, which can be traced through the left obturator foramen. The posterior arms are seen passing through the pararectal tissue (*arrows* in **c**). **d** The ischial spine (*IS*) is marked and the mesh can be followed as it comes around the rectum (*R*) heading to the sacrospinous ligament (*S*). 3D reconstruction of the pubic bone (**e, f**) was based on the *blue* tracing on **c** and **d**

Results

Patients

Three post-menopausal patients with a cystocele (paravaginal defect, which was clinically diagnosed as the descent of the lateral vaginal sulcus) and POP-Q state III were treated with an anterior mesh repair and an additional POP-Q stage I–II rectocele with posterior colporrhaphy. The complete surgical procedures were performed by two expert urogynecological surgeons (surgical experience > 10 years) according to the company recommendations for mesh implantation. Patient A (67 years old) and patient C (74 years old) both received a Seratom E PA MR implant and patient B (66 years old) a Seratom P PA MR implant. Hysterectomy was not carried out in any of the three cases. All operations were performed without complications. The patients were discharged approximately 48 h after surgery. The 12-week post-surgical gynecological assessment showed a good local healing process with no mesh erosion, dyspareunia or POP recurrence in any of the treated compartments. POP grading under Valsalva maneuver was determined to be grade 0–I in all patients.

Mesh visualization on MRI

The MRI-visible mesh including all six arms could be identified on all three patients' post-surgical T1w MRI. Sample images of three axial MRI sequences at the level of the arcuate pubic ligament and ischial spine level of one patient are shown in Fig. 2. The mesh is best seen on T1w images whereas traditional T2w images were best for identifying anatomical structures (Fig. 2). T1w fl3D sequences provide superior contrast and details for mesh visualization to T1w fl2D images owing to the thin slices, which had less of a spatial averaging effect (Fig. 2). No post-operative complications such as free fluid, seroma or hematoma were present on MRI and the pelvic organs were shown without pathological findings.

Mesh 3D reconstruction and its relationship to important anatomical structures

A reconstruction of each implanted mesh was feasible using the 3D-Slicer® in all three subjects, including both the main body of the mesh and each arm (Fig. 3). In addition, adjacent structures such as the sacrospinous ligament and the pudendal

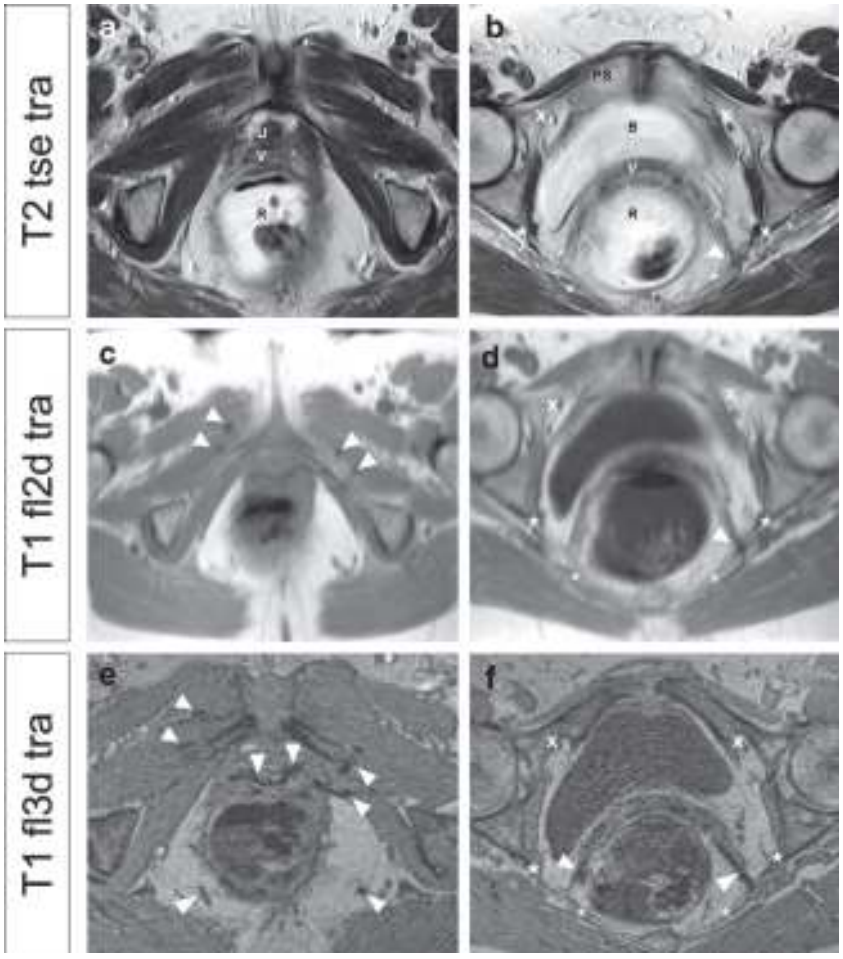

Fig. 2 Comparison of three MRI sequences at two levels (*left*, urethra; *right*, bladder). **a, b**: T2-weighted turbo spin echo sequence with 5-mm slice thickness. **c, d** T1w fl2D sequence with 6-mm slice thickness. **e, f** T1w fl3D sequence with a 1-mm slice thickness. Note that the T2w images best visualize the soft-tissue contrast for morphological information; however, the mesh is best seen on T1w images owing to the artifacts of the iron components (*arrows*). The thin mesh structure can best be seen using thin-sliced T1w fl3D. *tra* transverse, *U* urethra, *V* vagina, *PS* pubic symphysis, *B* bladder, *R* rectum; *asterisk* sacro-uterine ligament, *star* ischial spine, *x* obturator foramen

and obturator nerve could be identified and displayed. The location of the main body of the anterior mesh is seen between the bladder/bladder neck and the anterior vaginal wall (Fig. 2, Supplementary material). All six arms could be reconstructed in the full course from the main body to and through the pelvic sidewalls, sacrospinous ligament area, and ischio-rectal fossa, demonstrating their course via either the obturator foramen (anterior and middle arms) or the sacrospinous ligament (posterior arms; Fig. 3, Supplementary material). The 3D spatial relationship between mesh and important anatomical structures such as the obturator vessel and pudendal nerve vessel bundles can be appreciated in detail (Fig. 4).

Discussion

The results of this study demonstrate the feasibility of complete 3D mesh reconstructions after anterior vaginal mesh repair in living women using a, MRI-visible polypropylene mesh. The implanted Fe_3O_4 polypropylene mesh is visible in sufficient detail in all three cases so that the contour and mesh location could be identified and reconstructed. We used a point cloud-based technique instead of traditional 3D volume rendering technique to reconstruct the mesh [13], allowing for precise location identification of all visible parts of the mesh and avoiding lofting artifacts that can occur in volume (solid) model creation. This display enabled the following important relationships to be studied:

1. The anterior and middle arms through the obturator foramen with its relationship to obturator vessel nerve bundle
2. The posterior arms passing through the sacrospinous ligament in relationship to the pudendal vessel nerve bundle
3. The mesh body location relative to the vaginal wall and bladder/bladder neck

To date, studies published have shown the MRI visibility of mesh material experimentally, in a cadaver [9], rat models [11], and abdominal hernia reconstruction using polyvinylidene fluoride (PVDF) as matrix [10, 18–20], and only one study group using a MRI-visible PVDF mesh for pelvic floor reconstruction [13]. This report extends what has previously been reported in the literature by demonstrating the feasibility of using Fe_3O_4 polypropylene mesh in living women and reconstructing the 3D course of its body and arms in relationship to important anatomical landmarks. This is an extension of the cadaver work [9] to show that the healing process, and the movements of the organs during breathing and pulsatile movement of blood vessels in living women, do not prevent visualization of the fine mesh filaments.

Ultrasound has been widely used in the clinic and has demonstrated its capability to detect implanted meshes and help with the diagnosis of mesh complications. It demonstrates

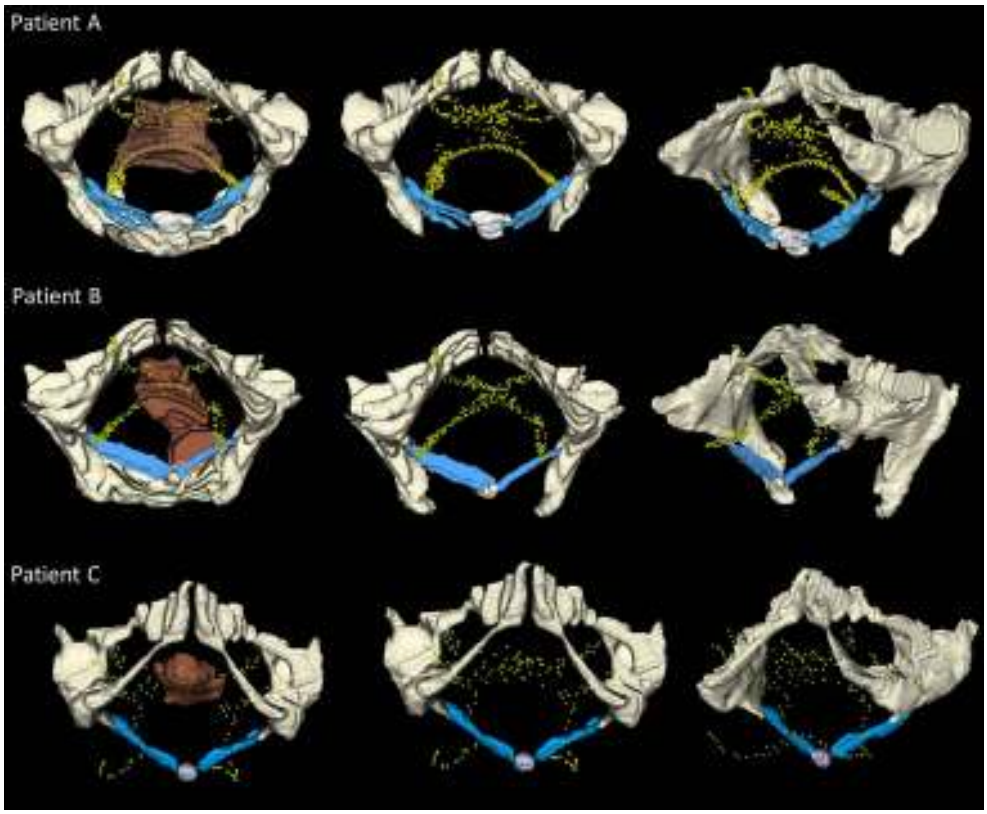

Fig. 3 3D models created from post-surgical MRI of all three patients. In the *left column* the reconstructed pelvic bones including the sacrum are demonstrated in addition to the vagina/uterus (*brown*), sacrospinous ligament (*blue*), and the MRI-visible mesh (*yellow dots*). The reconstruction software allows structures to be turned on or off as needed for evaluation. In the *middle column*, the vagina/uterus and sacrum (but not the coccyx) are hidden, for better illustration of the mesh placement in the pelvis. In the *right column*, the models are rotated to a three-quarter view revealing a different impression on how the left anterior and middle mesh arms are positioned in the obturator foramen or where the posterior arms pass through the sacrospinous ligament

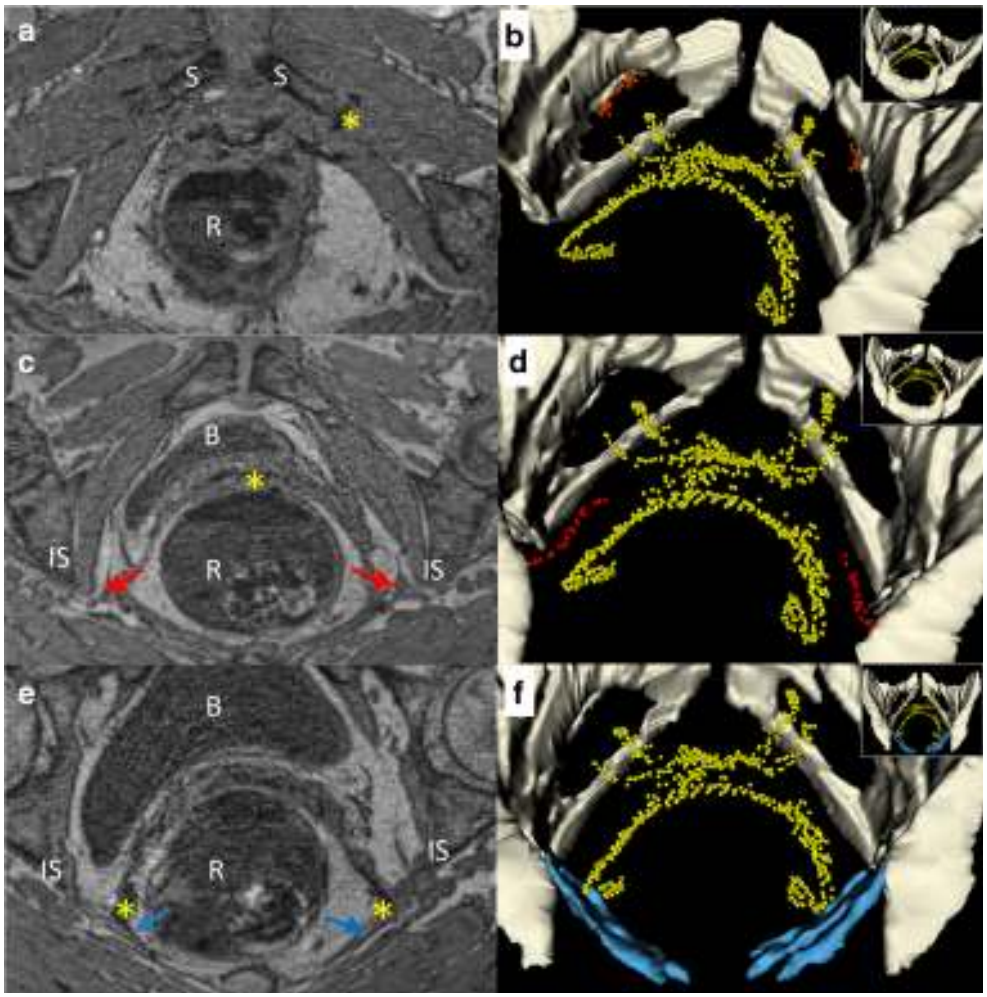

Fig. 4 MRI-visible mesh visualization and 3D reconstruction, demonstrating mesh placement in the pelvis and its spatial relationship with important anatomical structures in patient 1. **a**, **c** and **e** axial MRI (T1w fl3D sequence), mesh marked with *yellow asterisk*. **b** Into-out view of same patient's reconstructed 3D model of the pelvis and mesh. The anterior and middle mesh arms pass outward through the obturator foramen at a safe distance away from the obturator vessels (*red dots*). **c, d** 3D reconstruction shows the pudendal nerve vessel bundle (*red arrows* in **c** or dots in **d**) at an adequate distance from the mesh and its arms. **e, f** Penetration of the sacrospinous ligament (*blue arrows* in **e** and three-dimensionally reconstructed model (*blue area* in **f**)) by the posterior mesh arms at a safe distance from the pudendal nerve vessel bundle and ischial spine (*IS*). *B* bladder, *R* rectum, *S* symphysis

excellent visibility of segments of the mesh between the vagina and bladder [6] and has proven to be especially useful in diagnosing mesh folding or dislodgement [6] or in evaluating recurrent cystoceles after anterior colporrhaphy using alloplastic material [21, 22]. Because of its favorable cost/benefit ratio and the ability to effect real-time viewing, we believe that ultrasound will remain the mainstay for most clinical situations. However, the ultrasound technique has its limitations in evaluating the course of the mesh arms laterally in the pelvis and their relationship to adjacent structures near pelvic sidewalls because of the limited scope of the ultrasound volume. The combination of MRI-visible mesh and the fact that MRI can provide additional information in some circumstances justifies its higher cost, for example, perineal pain, which may originate in mesh irritation of the pudendal nerve, and leg pain, possibly caused by obturator irritation. In these circumstances, MRI-visible mesh and MRI can provide additional information by capturing the entire pelvic region, including the bony pelvis, soft-tissue structures, and implanted mesh simultaneously. Being able to follow the course of the mesh arms through deep pelvic structures, which cannot be reached by ultrasound, and demonstrate the 3D relationship between implanted mesh and important anatomical structures (e.g., pudendal nerve, obturator foramen), can help to detect and evaluate mesh-related complications (such as post-surgical pain and dyspareunia). MRI cannot replace clinical examination for the detection of the origin of neuropathic pain; however, MRI is able to depict anatomical changes close to the course of a specific nerve. Furthermore, if the mesh is located close to neurovascular structures, knowing where the vessels and the mesh are in 3D space can help the surgeon to stay out of the danger zone during revision surgery. In addition, unlike ultrasound, MRI is performed following a predefined protocol and is user-independent, allowing a reliable pre- and post-surgical comparison and long-term follow-up examinations with inter-subject comparison, without depending on the skills and experience of the ultrasound operator.

The interactive nature of 3D reconstructed models, with the free open source 3D Slicer® software or other model building programs, allows the physician to add or subtract anatomical structures or rotate the constructed 3D model according to

user-defined importance for better visualization of certain pelvic areas, and could be used to measure distances between the mesh and anatomical landmarks. It could be a useful feedback tool in an educational and clinical setting, allowing surgeons to visualize the complete mesh with MRI and re-evaluate their personal implantation technique. For example, on Figs. 1, 2, the distal portion of the mesh can be found beneath the proximal part of the urethra on MRI 3 months post-surgery, whereas the intended inferior-most location of mesh is at the bladder neck level by mesh designer and surgeon [23]. The evaluation of post-surgical mesh positioning may also help surgeons and mesh designers to optimize mesh dimensions and fixation strategies to provide sufficient support with fewest possible side effects. 3D visualization has been used by Larson et al., who compared manufacturer-specified placement of non-MRI-visible anterior wall mesh kits with 3D vaginal models in women with normal support [23]. Enhancing this information, the MRI-visible Fe_3O_4 polypropylene mesh and its 3D reconstruction in post-surgery MRI can provide a wider range of information for studying the mesh and its fixation behavior in living women than solely evaluating the clinical examination and ultrasound results. This could potentially lead to improved design or innovation to help decrease future mesh complications.

Several factors should be kept in mind when interpreting the results of this study. We recognize the small number of women examined, limiting a widespread data evaluation, and subsequent research is needed to determine how consistently the mesh can be seen. Despite the fact that we are of the opinion that this technique is very valuable for clinical life and forthcoming urogynecological research, we are aware of the time-consuming and expensive nature of MRI and 3D reconstruction in a normal clinical setting, limiting its use for more complicated cases.

The MRI-visible mesh allows the visualization of the mesh body and the course of the mesh arms. This technique allows the relationship between the mesh and adjacent muscular, bony, and neurovascular structures to be displayed and evaluated. Although we focused on the pelvic bones, sacrospinous ligament, and pudendal and obturator neurovascular bundles, the full complement of anatomical structures in and around the pelvis that can be seen on MRI could be modeled and examined in relationship to the mesh.

Conclusions

Magnetic resonance imaging of the MRI-visible mesh and its 3D reconstruction technique allows us to visualize the full course of the mesh, including both mesh body and mesh arms in relationship to important pelvic floor structures. It has promised to be a useful tool in assisting with evaluation of possible mesh complications, such as suspected neurovascular injury. It could also be a valuable interactive biofeedback tool for the surgeon. Furthermore, the technique allows the biomedical engineers to examine the mesh structure mechanics in living women, providing insights into optimizing future mesh design.

Acknowledgements We thank Dr A. Maleika (Director of the Department of Obstetrics and Gynecology, Hospital Schwetzingen, Germany) for her assistance in patient recruitment for this trial. Dr J. DeLancey and Dr L. Chen acknowledge support from the Office for Research on Women's Health Special Center of Research Grant at the NIH P50 HD 44406 and R21 HD079908.

Compliance with ethical standards

Financial disclaimers KAB and FL received speaking honoraria from the company Serag Wiessner (Naila, Germany). FL received speaking honoraria from American Medical Systems, USA, and C.R. BARD, Karlsruhe, Germany. No money from speaking honoraria was used to fund this trial. KAB has received research funding from Serag Wiessner in the past, none of which was used to perform this trial. KAB received a scholarship from the organization Forum urodynamicum e.V. to complete this work. CDA and CS state that they have nothing to disclose.

References

1. Boyles SH, Weber AM, Meyn L. Procedures for pelvic organ prolapse in the United States, 1979–1997. Am J Obstet Gynecol. 2003;188(1):108–15.
2. Olsen AL, Smith VJ, Bergstrom JO, Colling JC, Clark AL. Epidemiology of surgically managed pelvic organ prolapse and urinary incontinence. Obstet Gynecol. 1997;89(4):501–6.
3. Wu JM, Kawasaki A, Hundley AF, Dieter AA, Myers ER, Sung VW. Predicting the number of women who will undergo incontinence and prolapse surgery, 2010 to 2050. Am J Obstet Gynecol. 2011;205(3):230 e1–5.
4. Abed H, Rahn DD, Lowenstein L, Balk EM, Clemons JL, Rogers RG. Incidence and management of graft erosion, wound granulation, and dyspareunia following vaginal prolapse repair with graft materials: a systematic review. Int Urogynecol J. 2011;22(7):789–98.
5. Farthmann J, Watermann D, Niesel A, Funfgeld C, Kraus A, Lenz F, et al. Lower exposure rates of partially absorbable mesh compared to nonabsorbable mesh for cystocele treatment: 3-year follow-up of a prospective randomized trial. Int Urogynecol J. 2012;24(5):749–58.
6. Shek KL, Dietz HP, Rane A, Balakrishnan S. Transobturator mesh for cystocele repair: a short- to medium-term follow-up using 3D/4D ultrasound. Ultrasound Obstet Gynecol. 2008;32(1):82–6.
7. Dietz HP, Barry C, Lim YN, Rane A. Two-dimensional and three-dimensional ultrasound imaging of suburethral slings. Ultrasound Obstet Gynecol. 2005;26(2):175–9.
8. Tunn R, Albrich S, Beilecke K, Kociszewski J, Lindig-Knopke C, Reisenauer C, et al. Interdisciplinary S2k guideline: sonography in urogynecology: short version - AWMF registry number: 015/055. Geburtshilfe Frauenheilkd. 2014;74(12):1093–8.
9. Brocker KA, Lippus F, Alt CD, Hallscheidt P, Zsolt F, Soljanik I, et al. Magnetic resonance-visible polypropylene mesh for pelvic organ prolapse repair. Gynecol Obstet Invest. 2014;79(2):101–6.
10. Hansen NL, Barabasch A, Distelmaier M, Ciritsis A, Kuehnert N, Otto J, et al. First in-human magnetic resonance visualization of

surgical mesh implants for inguinal hernia treatment. Invest Radiol. 2013;48(11):770–8.
11. Kuehnert N, Kraemer NA, Otto J, Donker HC, Slabu I, Baumann M, et al. In vivo MRI visualization of mesh shrinkage using surgical implants loaded with superparamagnetic iron oxides. Surg Endosc. 2011;26(5):1468–75.
12. Fischer A. OP-Atlas Praktische Urogynäkologie. Berlin: Birgitt Lucas; 2007.
13. Sindhwani N, Feola A, De Keyzer F, Claus F, Callewaert G, Urbankova I, et al. Three-dimensional analysis of implanted magnetic-resonance-visible meshes. Int Urogynecol J. 2015;26(10):1459–65.
14. Brocker KA, Alt CD, Corteville C, Hallscheidt P, Lenz F, Sohn C. Short-range clinical, dynamic magnetic resonance imaging and P-QOL questionnaire results after mesh repair in female pelvic organ prolapse. Eur J Obstet Gynecol Reprod Biol. 2011;157(1):107–12.
15. Fedorov A, Beichel R, Kalpathy-Cramer J, Finet J, Fillion-Robin JC, Pujol S, et al. 3D Slicer as an image computing platform for the Quantitative Imaging Network. Magn Reson Imaging. 2012;30(9):1323–41.
16. Larson KA, Luo J, Yousuf A, Ashton-Miller JA, Delancey JO. Measurement of the 3D geometry of the fascial arches in women with a unilateral levator defect and "architectural distortion". Int Urogynecol J. 2012;23(1):57–63.
17. Chen L, Lisse S, Larson K, Berger MB, Ashton-Miller JA, DeLancey JO. Structural failure sites in anterior vaginal wall prolapse: identification of a collinear triad. Obstet Gynecol. 2016;128(4):853–62.
18. Ciritsis A, Truhn D, Hansen NL, Otto J, Kuhl CK, Kraemer NA. Positive contrast MRI techniques for visualization of iron-loaded hernia mesh implants in patients. PLoS One. 2016;11(5):e0155717.
19. Ciritsis A, Hansen NL, Barabasch A, Kuehnert N, Otto J, Conze J, et al. Time-dependent changes of magnetic resonance imaging-visible mesh implants in patients. Invest Radiol. 2014;49(7):439–44.
20. Kohler G, Pallwein-Prettner L, Koch OO, Luketina RR, Lechner M, Emmanuel K. Magnetic resonance-visible meshes for laparoscopic ventral hernia repair. JSLS. 2014;19(1):e2014.00175.
21. Wong V, Shek KL, Goh J, Krause H, Martin A, Dietz HP. Cystocele recurrence after anterior colporrhaphy with and without mesh use. Eur J Obstet Gynecol Reprod Biol. 2014;172:131–5.
22. Rodrigo N, Wong V, Shek KL, Martin A, Dietz HP. The use of 3-dimensional ultrasound of the pelvic floor to predict recurrence risk after pelvic reconstructive surgery. Aust N Z J Obstet Gynaecol. 2014;54(3):206–11.
23. Larson KA, Hsu Y, DeLancey JO. The relationship between superior attachment points for anterior wall mesh operations and the upper vagina using a 3-dimensional magnetic resonance model in women with normal support. Am J Obstet Gynecol. 2009;200(5):554 e1–6.